Experimental demonstration of particle energy, conversion efficiency and spectral shape required for ion-based fast ignition

2011 Nucl. Fusion 51 083011

(http://iopscience.iop.org/0029-5515/51/8/083011)

IOP Publishing and International Atomic Energy Agency Nuclear Fusion
Nucl. Fusion **51** (2011) 083011 (6pp) doi:10.1088/0029-5515/51/8/083011

Experimental demonstration of particle energy, conversion efficiency and spectral shape required for ion-based fast ignition

B.M. Hegelich[1,2], D. Jung[1,2], B.J. Albright[1], J.C. Fernandez[1], D.C. Gautier[1], C. Huang[1], T.J. Kwan[1], S. Letzring[1], S. Palaniyappan[1], R.C. Shah[1], H.-C. Wu[1], L. Yin[1], A. Henig[2], R. Hörlein[2], D. Kiefer[2], J. Schreiber[2], X.Q. Yan[2], T. Tajima[2], D. Habs[2], B. Dromey[3] and J.J. Honrubia[4]

[1] Los Alamos National Laboratory, Los Alamos, New Mexico 87544, USA
[2] Fakultät für Physik, Ludwig-Maximilian-Universität München, D-85748 Garching, Germany
[3] Department of Physics and Astronomy, Queens University Belfast, Belfast, BT7 1NN, UK
[4] USAETSI Aeronáuticos, Universidad Politécnica de Madrid, 28040 Madrid, Spain

E-mail: hegelich@lanl.gov

Received 28 February 2011, accepted for publication 3 June 2011
Published 7 July 2011
Online at stacks.iop.org/NF/51/083011

Abstract
Research on fusion fast ignition (FI) initiated by laser-driven ion beams has made substantial progress in the last years. Compared with electrons, FI based on a beam of quasi-monoenergetic ions has the advantage of a more localized energy deposition, and stiffer particle transport, bringing the required total beam energy close to the theoretical minimum. Due to short pulse laser drive, the ion beam can easily deliver the 200 TW power required to ignite the compressed D–T fuel. In integrated calculations we recently simulated ion-based FI targets with high fusion gain targets and a proof of principle experiment [1]. These simulations identify three key requirements for the success of ion-driven fast ignition (IFI): (1) the generation of a sufficiently high-energetic ion beam (≈400–500 MeV for C), with (2) less than 20% energy spread at (3) more than 10% conversion efficiency of laser to beam energy. Here we present for the first time new experimental results, demonstrating all three parameters in separate experiments. Using diamond nanotargets and ultrahigh contrast laser pulses we were able to demonstrate >500 MeV carbon ions, as well as carbon pulses with $\Delta E/E < 20\%$. The first measurements put the total conversion efficiency of laser light into high energy carbon ions on the order of 10%.

(Some figures in this article are in colour only in the electronic version)

1. Introduction

This paper summarizes significant recent progress, in experiments and modelling, towards the realization of high fusion gain using the fast ignition (FI) approach [2] to inertial confinement fusion (ICF), made possible by the invention of high-power (∼kJ), short pulse (<ps) lasers. Specifically, we discuss progress on the special ion-driven fast ignition (IFI) variant of this approach using laser-driven ion beams to ignite the fuel. Within the fast ignition concept, such a high-power (∼PW) laser is used to deliver sufficient power density ($\sim 10^{23}$ W cm^{-3}) to the DT fusion fuel at the time of stagnation at maximum compression (∼10 s of ps), to isochorically heat a spot in the fuel to ∼10 keV.

1.1. Electron fast ignition (EFI)

The standard (electron based) variant of fast ignition seeks to deliver the energy via fast electrons (∼MeV), accelerated in the laser–fuel interaction [3, 4]. To overcome challenges of laser-beam transport to the dense fuel core regions, this scheme was later modified by the addition of a re-entrant cone to ensure laser–plasma interaction close to the compressed core [5], but beam transport through plasma due to prepulse induced

cone filling and electron transport to the hot spot due to large divergence of the electron beam remain the key challenges for electron fast ignition.

1.2. Proton fast ignition (PFI)

A possible alternative became feasible with the demonstration of proton acceleration from high power lasers at the petawatt laser at Lawrence Livermore National Laboratory (LLNL). Using the so-called 'target normal sheath acceleration' (TNSA) mechanism [6], LLNL was able to accelerate protons to up to 60 MeV in an exponential spectrum [7]. Together with excellent emittance of the ion beam [8, 9], which enables ballistic focusing via a shaped target [10], laser-driven electrostatic lenses [11] or miniature magnetic quadrupoles [12] to micrometre focal sizes, this in principle enables its use as a fast ignitor, first suggested by Roth *et al* in 2002 [13] and refined since then [14, 15]. The main challenges of the proton fast ignition (PFI) concept as currently envisioned lie (a) in the Maxwellian nature of the TNSA produced proton spectra, (b) the low particle energy and (c) the relatively low demonstrated conversion efficiencies of laser-light into protons. (A) spectral shape: the non-monoenergetic nature of the proton spectrum causes significant time-of-flight spread in the proton beam over longer distances and therefore requires the proton source to be situated close (∼1 mm) to the target, in turn requiring re-entrant cones and protection foils with all of the added complications of target design, laser transport and particle transport. (B) particle energy: the required particle energies for proton fast ignition are in the range 5–15 MeV to achieve stopping at the right range in the fuel. Since the energy per particle is low, a very large number of protons ($>10^{16}$) is required to carry the necessary energy of ∼10 kJ. From current experiments it is not yet clear if such a large number of protons can be supported by the proton target and efficiently accelerated by the laser. (C) conversion efficiency: demonstrated conversion efficiencies for proton acceleration are currently at the 1–3% level, requiring several hundred kJ to MJ lasers to produce the required 10 kJ of protons. Such a system would not represent significant savings over a standard (non-FI) IFE facility at the MJ level. Efficiencies of at least 10% are required to make any of the FI concepts feasible.

1.3. Ion fast ignition (IFI)

Using heavier ions than protons to achieve ignition is advantageous primarily due to the stiffer transport characteristics of a heavy ion beam and the enhanced stopping power of heavier ions, which would allow a much more precise deposition of all of the energy in the hotspot volume [16, 17]. Furthermore, due to the increased stopping, the particle energy to penetrate a given plasma to a specific depth has to be higher than for protons, meaning each particle will deliver more energy, allowing the total number of particles to be a lot smaller. This in principle eases a lot of target design problems. Our recent simulations were able to identify the key parameters for a carbon-based fast ignition scheme: on the order of 10^{14} carbon ions with energies of $\sim 440 \pm 50$ MeV or 37 MeV/nucleon have to be focused into the $\sim 20\,\mu m^3$ hot spot [1, 18]. However, exactly these characteristics make TNSA based IFI impossible. Due to their enhanced stopping heavier ions not only benefit from, but require a monoenergetic spectrum, albeit a fairly broad one ($\Delta E/E \sim 20\%$). While efficient TNSA acceleration for heavier ions has been demonstrated [19, 20], obtaining a sufficiently narrow carbon spectrum using the TNSA mechanisms has been shown only at lower efficiencies of ∼0.1% [21], which makes it infeasible for ion fast ignition. However, the recent discovery of new ion acceleration mechanisms in large-scale PIC simulations has changed this paradigm. Specifically, the break-out afterburner (BOA) mechanism [22, 23] and radiation pressure acceleration (RPA) [24, 25] seem to be well suited to deliver the required parameters for ion fast ignition. In contrast to TNSA, these variants of light pressure acceleration act predominantly on the high-Z ions, transferring most the laser energy to the high-Z ions rather than the protons, making them ideal candidates for IFI. The challenge is in the experimental realization of these mechanisms: to reach the required regimes on current laser systems, that are 2–3 orders of magnitude smaller than a full FI laser, requires ultrathin (∼nm) targets and therefore ultrahigh contrast of the laser pulse. Until recently, these requirements were out of range for all existing laser facilities. However, with the recent ultrahigh contrast upgrade of the Trident laser [26] and the development of robust, free-standing ultrathin diamond-like carbon (DLC) foils at LMU Munich, we could now conduct a first series of experiments to investigate the feasibility of ion fast ignition.

2. Experimental setup

2.1. Laser system and contrast

The experiments were performed at the Trident laser at Los Alamos National Laboratory (LANL) [27]. The shortpulse arm of the Trident laser delivers routinely 80 J on target with a pulse duration of 500–600 fs in a 1.5 × diffraction limited spot using an $F/3$ off-axis parabola, resulting in an average spot intensity of $\sim 2 \times 10^{20}\,W\,cm^{-2}$ and a peak intensity of $\sim 5 \times 10^{20}\,W\,cm^{-2}$. Trident employs a nonlinear filter technique to improve its pulse contrast [28], which is a key parameter for all chirped pulse amplification systems (CPA) [29]. The contrast describes how fast the pulse turns on. Due to the nature of CPA, where a short sub-ps laser pulse is stretched in time (ns) then amplified and then recompressed to its original short duration, the short high intensity pulse sits on a ns pedestal of incompressible noise. In addition reflections in the system can also cause short prepulses before the main pulse and imperfect stretching/compression will induce ps 'shoulders' into the pulse shape. The laser contrast is the ratio of the pedestal/prepulse intensity at a given point in time to the peak intensity of the main pulse. For a typical ultrahigh intensity system that ratio is on the order of one millionth (10^{-6}) at ∼1 ns before the 500 fs main pulse. If the focused main pulse intensity is $\sim 10^{20}\,W\,cm^{-2}$, the prepulse intensity will be $\sim 10^{14}\,W\,cm^{-2}$, i.e. more than enough to create a plasma and to destroy the target before the main pulse can interact with it. For the advanced ion acceleration schemes to work at $10^{20}\,W\,cm^{-2}$ intensities, it is imperative that the initially only 5–50 nm thick target is still overdense at the peak of the pulse. Therefore, at peak intensities above $10^{20}\,W\,cm^{-2}$ very good contrast ratios of better than 10^{-12} at ∼ns are required. To realize

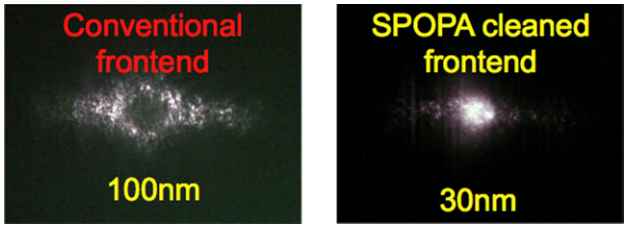

Figure 1. Full backscatter images from 100 nm and 30 nm targets shot with the conventional and ultrahigh contrast system, respectively.

these extreme, ultrahigh contrast conditions, we developed a new cleaning system based on short pulse optical parametric amplification (SPOPA) [26]. Using an additional compressor stretcher pair and exploiting two quadratic nonlinearities we obtain cubic cleaning performance at great stability at modest intensity, realizing a contrast good enough to ensure main pulse interaction with an overdense target. The thus realized contrast currently is below the detection threshold of our optical diagnostics at 0.5 ns. Damage threshold measurements on the used targets put it as low as $<2 \times 10^{-12}$ for a 1.2 ns pedestal and $<5 \times 10^{-10}$ for 0.5 ps prepulse. Closer in the contrast is measured to be $<10^{-9}$ @ 50 ps and $< 10^{-7}$ @ 5 ps. Figure 1 shows the full aperture backscatter images of a 100 nm target shot with the old frontend and contrast of $\sim 10^{-7}$ @ ns and a 30 nm target shot with the improved contrast values. Whereas the 100 nm target shows a clear hole in the centre, burned through by the prepulse, the 30 nm target shows a strong central reflection from an overdense plasma. Targets as thin as 3 nm were successfully shot on Trident, remaining overdense during a large part of the interaction.

2.2. Targets

The second requirement to successfully reach the BOA/RPA regime at $\sim 10^{20}$ W cm^{-2} is nanometre targets. We employed nanometre-thin DLC foils, developed at the Kurchatov Institute in Moscow and perfected for this application and produced at LMU Munich using a specialized cathodic arc discharge [30]. DLC is a metastable form of amorphous carbon. Due to their high content of sp3 bonds, 50–75% for the targets used, the foils possess an exceptional mechanical robustness. Furthermore they are very transparent, making them less susceptible to laser prepulses, resulting in a high optical damage threshold.

2.3. Diagnostics

The Trident North Target Area was used for the experiments and a variety of different diagnostics was employed simultaneously. The exact diagnostics setup changed and evolved over the four experimental campaigns but a typical setup is shown in figure 2. The main diagnostics consists of a suite of Thomson parabola ion spectrometer at different angles, ranging from compact low resolution spectrometers to a next generation, high resolution Thomson parabola specifically developed for these experiments [31], with an energy resolution of >2 GeV for carbon ions and charge state resolution C^{6+}/C^{5+} at >1 GeV. The Thomson parabolas are typically fielded at 1–2 m distance from the target using 100–300 μm pinholes, resulting in a solid angle of $\sim 10^{-7}$–10^{-8} sr. As a secondary diagnostic several compact electron spectrometers are employed at different angles with energy resolution in the 10–100 MeV range. To analyse the pulse transmitted through the target during relativistic transparency (see below) we use a optical spectrometer, a single shot second order autocorrelator and a specially developed single shot FROG device [32].

3. Experimental results

To date, five experimental campaigns investigating laser-driven ion acceleration for ion fast ignition have been conducted on the Trident laser. Interacting the Trident laser pulse at normal incidence with a range of different thickness DLC targets, the optimal target parameters for Trident conditions could be determined, resulting in a first demonstration of >0.2 GeV carbon ions accelerated by a <40 J, 700 fs, 7×10^{19} W cm^{-2} laser pulse, using double plasma mirrors for contrast enhancement [33]. The four subsequent beam times using the SPOPA instead of double plasma mirrors and therefore $\sim 2 \times$ the pulse energy demonstrated repeatedly carbon energies above 0.5 GeV, as shown in figure 3 [34]. This range of experimental data and the comparison with large-scale 2D and 3D simulations using our VPIC code on the LANL Roadrunner supercomputer led to a detailed understanding of the underlying physics [34] and the development of a reduced analytical model [35]. When the laser pulse hits an overdense nanometre target, it heats up the target electrons while the target starts to expand. If the laser and target parameters are chosen correctly, the electrons will heat faster than the target is expanding, resulting in the condition $n_e/\gamma \; n_{cr} \; 1\sim$, with $n_e \gg n_{cr}$. Here, n_e is the electron density, n_{cr} the critical density for the laser wavelength and γ is the relativistic gamma factor of the electrons. In such a situation the target becomes relativistically transparent though still classically overdense, and the laser can penetrate the target and propagate within, volumetrically interacting with all target electrons. This leads to coherent, laser-driven electron motion, which sets up charge separation fields and kinetic instabilities with the slower ion population that can effectively transfer energy from the electrons to the ions [36]. The energy lost by the electrons is immediately replenished by the superimposed laser field, making this mechanism very efficient for ion acceleration.

3.1. Ion energies

At the optimal thickness for Trident conditions, between 50 and 200 nm, we were able to demonstrate energies as high as 500 MeV, i.e. the required energies for IFI. Figure 3 shows typical examples of carbon 6^+ ion spectra obtained from the interaction of the Trident laser pulse ($E_{laser} \sim 80$ J, $\tau \sim 600$ fs, $d_{focus} \sim 7\,\mu$m FWHM) with a 150 nm thin diamond-like carbon foil ($\rho \sim 3$ g cm^{-3}). The laser was incident normal onto the target, i.e. the laser direction and target normal are parallel and designated 0°. The spectra were measured using three different Thomson parabola spectrometers fielded at angles of 0°, 22.5° vertical and 22.5° horizontal with respect to the laser axis and the target normal, as shown in figure 2. The

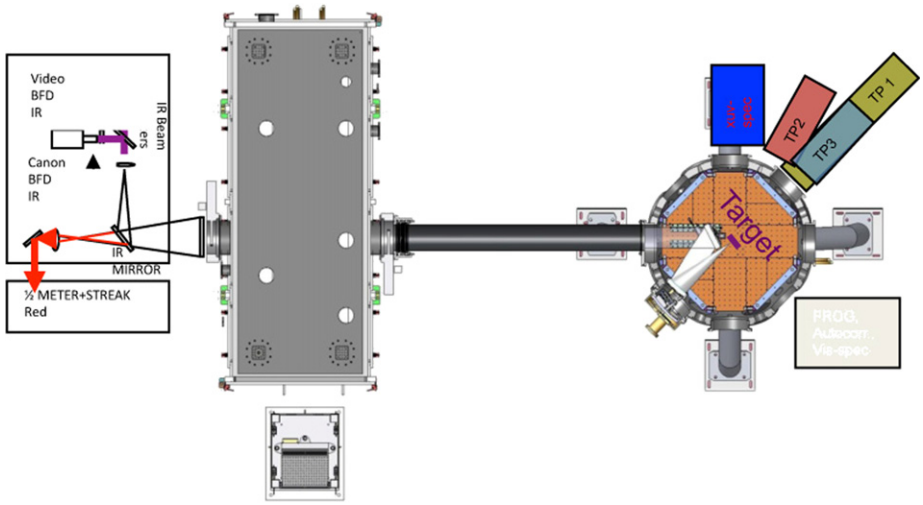

Figure 2. Typical experimental setup for ultrathin foil experiments on Trident: the target chamber (right) is outfitted with a variety of particle and optical diagnostics. A second diagnostic station to analyse the backscattered light is setup on the other side of the pulse compressor, looking at leakage of backscattered light through the compressor mirror with imaging and spectroscopical diagnostics.

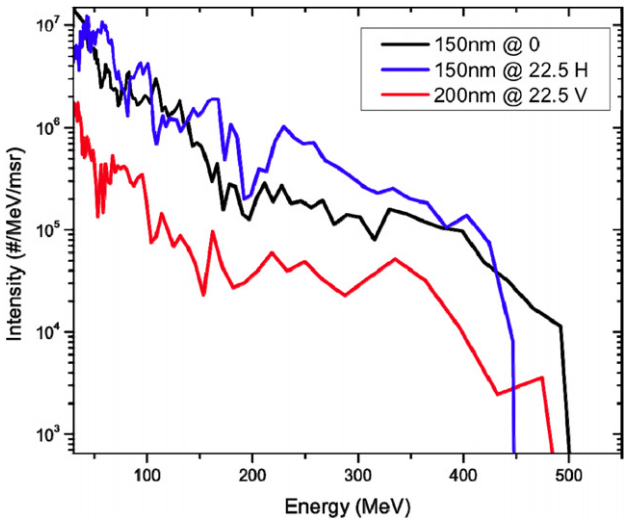

Figure 3. Laser-accelerated carbon spectra for optimal DLC target thickness for Trident conditions. The spectra are measured at different angles with respect to the laser (and target normal) direction: 0° (black), 22.5° vertical (red) and 22.5° horizontal (blue).

spectra show an exponential decaying distribution, with a real (not instrument induced) low energy cutoff, a remnant from a monoenergetic shape in an earlier acceleration phase. The highest energies and particle numbers are always observed for the 6^+ charge states. Other charge states, if they are present at all, typically show 2–3 orders of magnitude lower numbers and an order of magnitude lower particle energies. Using multiple Thomson parabolas, we could verify an approximate beam half angle of ∼25°, after which the energy declines steeply. The beam angle is related to the used focusing optics ($F/3$) and observed to decrease with a slower ($F/8$) optic and predicted to increase with a faster F/1 optic by simulations and theory.

3.2. Conversion efficiency

Preliminary estimates of laser energy to ion energy conversion efficiency ε can be done under the assumption of a homogeneously distributed beam within a 22.5° cone angle, as suggested by the measured ion spectra. Integrating the energy contained in the spectra in an energy range from 20 to 300 MeV, i.e. underestimating the total converted energy, we arrive at a figure of approximately ∼10%, depending on the exact shot conditions. This is the right order of magnitude for ion fast ignition, achieved under conditions far from optimal. PIC simulations suggest that temporal and spatial pulse shaping will improve both the efficiency as well as the spectral distribution of the ion beam. Similar efficiencies were obtained in measurements at the Max-Born-Institute in Berlin, using a much small Ti : sapphire laser with 0.7 J, 45 fs, 5×10^{19} W cm^{-2} and correspondingly thinner, 5 nm targets [37]. Whereas the Trident experiments are the first experimental demonstration of the BOA regime, here the first onset of RPA acceleration could be observed [38].

3.3. Spectral shape

The spectra shown in figure 3 show only weak remnants of monoenergetic shapes in their dropping low energy side and a slight increase/plateau at the high energy end. Obviously they are nowhere close to the required <20% energy spread for fast ignition. This is mainly due to the fact that we need every bit of laser intensity to achieve the 500 MeV required energies. Since a real fast ignition laser has to be orders of magnitude larger for pure energetics reasons, this allows us to trade of some of the intensity for spectral shaping. As we could show in experiments, the use of circular polarization can lead to more monoenergetic spectra. An example of this is shown in figure 4 and more detailed experimental data are published separately [39]. By reducing the initial target expansion it is possible to seed a tight ion density spike, an ion-soliton (discussed in the next section), which will keep its distribution of accelerating electrons during the BOA phase and thus preserve local charge neutrality, preventing its dispersion.

A different example of how such a spectrum can be obtained is shown in figure 5. Here we use a long focal length off-axis parabola ($F/8$), projecting a larger focal spot. This

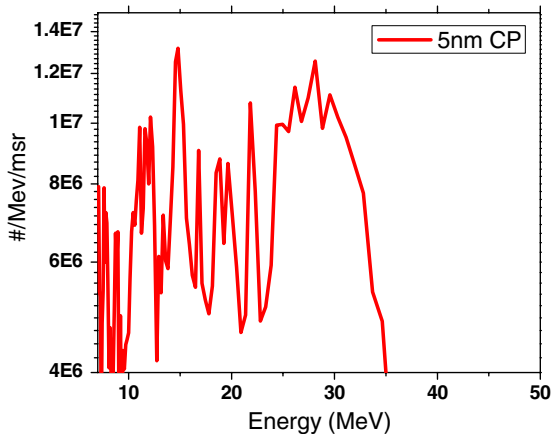

Figure 4. Monoenergetic feature in carbon C^{6+} spectrum from a 5 nm DLC target shot with circular polarization (ion soliton).

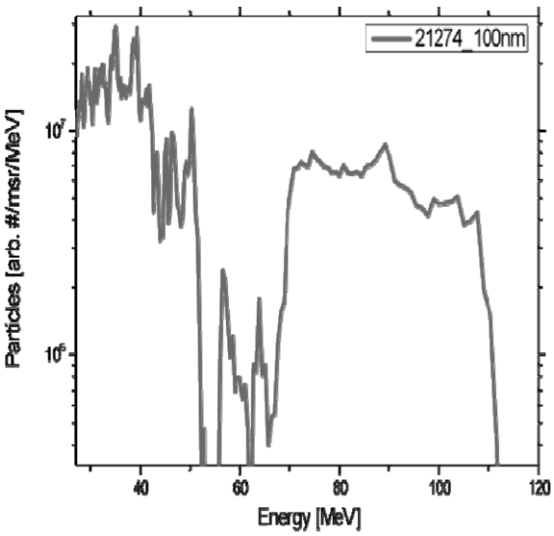

Figure 5. Monoenergetic carbon spectrum from BOA acceleration using a $F/8$ long focal range off-axis parabola.

reduces the on-target intensity and therefore the initial target expansion as well as the maximum ion energies. However, due to the longer Raleigh range the interaction length increases, off-setting the effect on maximal energies slightly. We obtain a peaked ion spectrum at 90 MeV mean energy with an energy spread of roughly 20%, i.e. in the ballpark of ion fast ignition. Narrower energy spreads (at ∼40 MeV) could be obtained using circular polarization and will be published separately [39]. A further way to achieve the spectral shaping observed in simulations is the use of double-foil targets, where a second foil behind the source foil acts as a beam stop for the tail of the laser pulse, preventing further heating of the co-propagating electrons. Furthermore, it swaps those electrons for colder electrons from the bulk of this second foil, reducing the space charge effects considerably and, last but not least, can set up a TNSA field acting as a bunch compressor if the parameters are chosen correctly. All three effects have the potential to further reduce the energy spread considerably [40, 41].

3.4. Soliton dynamics

The formation and propagation of ion solitons, an extension of Akhiezer–Polovin [42] dynamics to accommodate ion dynamics, has been considered in [34]. These dynamics begin at the time the target turns relativistically transparent and evolve via solitary waves with a sharp spike in ion density and a bipolar longitudinal electric field across the soliton, a characteristic structure that propagates self-similarly at a speed u_s that is comparable to the local ion longitudinal velocity. At the soliton interface, no corresponding electron density spike exists because the electrons are insufficiently mobile in the laser fields as to enable them to short out the electric field. Consequently, the electrical currents supporting the soliton are provided by the ions.

The free energy accelerating particles in the soliton come from the laser field in the following way: a circularly polarized laser propagating in plasma obeys the wave equation in the Coulomb gauge

$$\left(c^2\nabla^2 - \frac{\partial^2}{\partial t^2} - \frac{\omega_{\mathrm{pe}}^2}{\gamma_{\mathrm{e}}}\right)\vec{A} = 0,$$

where $\omega_{\mathrm{pe}}^2 = 4\pi n_{\mathrm{e}} e^2/m_{\mathrm{e}}$, $\gamma_{\mathrm{e}} = [1 + p_{\mathrm{e}}^2/m_{\mathrm{e}}^2c^2]^{1/2}$, and $\boldsymbol{A}$ is the vector potential of the laser field. As electrons approach the soliton, they accelerate in the longitudinal electric field of the soliton, thus increasing their parallel momentum and, consequently, their Lorentz factor. This variation in γ_{e} leads to a slight shift in index of refraction across the soliton. In kinetic simulations of the soliton dynamics [34], this change appears as a slight decrease in the laser amplitude across the ion density spike, associated with a partial reflection of the laser light (i.e. a transfer of laser momentum into electron longitudinal momentum). However, the variation in $|A|$ induces a longitudinal electrostatic field in the soliton through

$$\left(\frac{\partial}{\partial t} + v_{ez}\frac{\partial}{\partial z}\right)p_{ez} = e\frac{\partial\phi}{\partial z} - \frac{e^2}{2m_{\mathrm{e}}c^2\gamma_{\mathrm{e}}}\frac{\partial(|A|^2)}{\partial z},$$

the longitudinal projection of the electron momentum equation.

In other words, the soliton ion density spike gives rise to a longitudinal electric field, which changes the electron parallel momentum (and thus Lorentz factor) across the soliton. This variation reflects some of the laser light from the soliton, leading to enhancement of the electrostatic field further accelerating the ions and sharpening the ion density spike. As the soliton propagates, it slowly increases in speed, as seen in figure 4 of [34]; this process continues until the soliton breaks out of the back of the ion layer.

4. Conclusion

Recent experiments have for the first time shown the successful exploitation of the transparent-overdense regime of break-out afterburner acceleration. In the course of the experiments we demonstrated carbon energies from laser-accelerators as high as 500 MeV/nucleon at laser-to-ion energy conversion efficiencies approaching 10%. We could further demonstrate spectral shaping in the 20% $\Delta E/E$ range by a variety of mechanisms, e.g. circular polarization or spatial pulse shaping.

All pulse shaping methods employed today reduce the intensity on target, leading to lower energies for the demonstrated monoenergetic spectra. However, since a real fast ignition laser has to be many orders of magnitude more powerful due to simple energetics requirements this does not present a conceptual problem. These results demonstrate three of the four key requirements of ion-based fast ignition, leaving only focusing left. The next grand challenge will be to unify all the separate characteristics in one beam. The recent experimental progress on laser-driven ion acceleration enabled us to considerably advance the theory, too, and develop a reduced model that is in excellent agreement with both experiments and simulations. This model enables rapid-turn-around design estimates for future experiments and massively parallel three-dimensional PIC simulations requiring weeks of runtime on thousands of cores. Being able to optimize initial conditions for both enables a steady progress in understanding and optimization of the ion source. We can thereby identify the temporal and spatial pulse parameters required to successfully obtain all three beam parameters at once. In the worldwide absence of a laser system fulfilling all required parameters at once, we have therefore performed numerical experiments using our benchmarked and validated VPIC code to show that it is indeed possible to laser-accelerate carbon ions that will fulfil all three requirements simultaneously. These results are paving the way for a suitable, quasi-monoenergetic ignitor ion beam, which in turn enables feasible and much simpler targets that do not require a capsule with a reentrant cone. Ion-based FI is emerging as the variant with the most separability of its basic elements: (1) DT fuel compression to a mass density $\rho = 300$–$500\,\mathrm{g\,cm^{-3}}$, areal density $\rho r \approx 3\,\mathrm{g\,cm^{-2}}$; (2) generation of a ∼10 kJ, ∼450 MeV, quasi-monoenergetic ignitor carbon beam, achieved via the interaction of a high-power, high-energy short-pulse laser with a nano-target that is well separated from the imploded fuel capsule, and (3) the deposition of the beam energy in a relatively small 'hot spot' volume ($\sim 25\,\mu\mathrm{m}^3$), within $\tau \sim 20$–50 ps, which ignites the fuel. In addition to the obvious engineering advantages, this separability enables more rapid and cost-effective scientific progress and development in each area. With the recent progress in both theory and experiments, ion-based fast ignition can be considered as a serious alternative to the classical FI concepts.

Acknowledgments

We acknowledge the expert support of the Trident laser team (R. Johnson, T. Shimada, T. Hurry, R. Gonzales, S.-M. Reid, F. Archuleta). We also acknowledge K. Flippo's help in setting up the backscatter measurements and P. Hiltze's (LMU) support for target fabrication. This work is sponsored by the US DOE and the LANL LDRD program office and by the German DFG and LMUexcellent.

References

[1] Fernandez J.C. *et al* 2009 *Nucl. Fusion* **49** 065004
[2] Tabak M., Hammer J., Glinsky M.E., Kruer W.L., Wilks S.C., Woodworth J., Campbell E.M., Perry M.D. and Mason R. 1994 *J. Phys. Plasmas* **1** 1626
[3] Wilks S.C. *et al* 1992 *Phys. Rev. Lett.* **69** 1383
[4] Beg F.N. *et al* 1997 *Phys. Plasmas* **4** 447
[5] Kodama R. *et al* 2001 *Nature* **412** 798
[6] Hatchett S. *et al* 2000 *Phys. Plasmas* **7** 2076
[7] Snavely R. *et al* 2000 *Phys. Rev. Lett.* **85** 2945
[8] Schreiber J. *et al* 2004 *Appl. Phys.* B **79** 1041
[9] Cowan T. *et al* 2004 *Phys. Rev. Lett.* **92** 204801
[10] Patel P.K. *et al* 2003 *Phys. Rev. Lett.* **92** 125004
[11] Toncian T. *et al* 2006 *Science* **312** 410
[12] Schollmeier M. *et al* 2008 *Phys. Rev. Lett.* **101** 055004
[13] Roth M. *et al* 2001 *Phys. Rev. Lett.* **86** 436
[14] Atzeni S., Temporal M. and Honrubia J.J. 2002 *Nucl. Fusion* **42** L1
[15] Temporal M., Honrubia J.J. and Atzeni S. 2002 *Phys. Plasmas* **9** 3098
[16] Fernandez J.C. *et al* 2008 *J. Phys.: Conf. Ser.* **112** 022051
[17] Shmatov M. 2007 *Fusion Sci. Technol.* **52** 116
[18] Honrubia J.J. *et al* 2009 *Phys. Plasmas* **16** 102701
[19] Hegelich B.M. *et al* 2002 *Phys. Rev. Lett.* **89** 085002
[20] Hegelich B.M. *et al* 2005 *Phys. Plasmas* **12** 056314
[21] Hegelich B.M. *et al* 2006 *Nature* **439** 441
[22] Yin L. *et al* 2006 *Lasers Part. Beams* **24** 291
[23] Albright B.J. *et al* 2007 *Phys. Plasmas* **14** 094502
[24] Macchi A. *et al* 2005 *Phys. Rev. Lett.* **94** 165003
[25] Robinson A.P.L. *et al* 2008 *New J. Phys.* **10** 013021
[26] Shah R. *et al* 2009 *Opt. Lett.* **34** 2273
[27] Batha S.H. *et al* 2008 *Rev. Sci. Instrum.* **79** 10F305
[28] Wang Y. and Luther-Davies B. 1994 *J. Opt. Soc. Am.* B **11** 1531
[29] Mourou G.A. and Umstadter D. 2002 *Sci. Am.* 286
[30] Liechtenstein V.K. *et al* 1997 *Nucl. Instrum. Methods Phys. Res.* A **397** 140
[31] Jung D. *et al* 2011 *Rev. Sci. Instrum.* **82** 013306
[32] Palaniyappan S. *et al* 2010 *Rev. Sci. Instrum.* **81** 1
[33] Henig A. *et al* 2009 *Phys. Rev. Lett.* **103** 045002
[34] Yin L. *et al* 2011 *Phys. Plasmas* **18** 053103
[35] Yan X. *et al* 2010 *Appl. Phys.* B **98** 711
[36] Yin L. *et al* 2007 *Phys. Plasmas* **14** 056706
[37] Steinke S. *et al* 2010 *Laser Part. Beams* **28** 215
[38] Henig A. *et al* 2009 *Phys. Rev. Lett.* **103** 245003
[39] Jung D. *et al* 2011 Monoenergetic ion beam generation by driving ion solitary waves with circularly polarized laser light *Phys. Rev. Lett.* submitted
[40] Huang C. *et al* 2011 *Phys. Plasmas* **18** 056707
[41] Huang C. *et al* 2011 *Phys. Rev. ST Accel. Beams* **14** 031301
[42] Akhiezer A.I. and Polovin R.V. 1956 *Sov. Phys.—JETP* **3** 696